Time-evolution of the structure of organoclay/ polypropylene nanocomposites and its influence on time/temperature superposition principle

Riadh Zouari, Trystan Domenech, Edith Peuvrel-Disdier, Bruno Vergnes

Time-Evolution of the Structure of
Organoclay/ Polypropylene Nanocomposites
and its Influence on Time/Temperature Superposition Principle

R. Zouari, T. Domenech, E. Peuvrel-Disdier*, B. Vergnes*

MINES ParisTech, Centre de Mise en Forme des Matériaux (CEMEF),
UMR CNRS 7635, BP 207, 06904 Sophia-Antipolis Cedex (France)

*Corresponding authors: edith.disdier@mines-paristech.fr, bruno.vergnes@mines-paristech.fr

Abstract. We investigate the rheological properties of a nanocomposite in small amplitude oscillatory shear. The evolution of the storage modulus with time shows that this material is not stable: the microstructure changes continuously with time, due to the disorientation of the clay platelets and the build-up of a 3D network. This evolution of the microstructure is evaluated by measuring the apparent yield stress. A two-step kinetics is evidenced, whose parameters directly depends on temperature. This time-evolution is generally assumed to violate the time-temperature superposition principle. However, we demonstrate that the time-temperature equivalence always exists if we consider samples having the same microstructure.

Introduction

Although nanocomposite materials received a lot of interest in the last years, the exact nature of the nanocomposite structure is still an open question. Depending on the nanoclay state (from intercalated to fully exfoliated), the rheological behavior lies between a liquid-like and a solid-like one. The solid-like behavior is associated to the presence of a 3D structure where the nanoclay platelets and tactoids form a more or less soft network. Moreover, this microstructure can change with time or temperature, which renders the comprehension of the system complicated.

To our knowledge, studies dealing with time evolutionary nanostructured materials did not mention any time-temperature equivalence. However, some authors [1-3] found some failures by applying time-temperature superposition (TTS), principally in the low frequency range, and others [4-6] mentioned that the structure change within the nanocomposite leads to a violation of the TTS principle.

The aim of the present work is to study the development of the microstructure during an annealing process and to check the applicability of TTS principle. The conditions for a successful application of the TTS principle will be presented as well as information about the mechanisms leading to the formation of a 3D network within the polymer matrix.

Experiments

Materials. The organoclay is an organomodified montmorillonite (OMMT) (Dellite® 67G, provided by Laviosa Chimica Mineraria, Italy). The polymer matrix is an isotactic polypropylene (PP) (Moplen HP400R, provided by LyondellBasell). A polypropylene grafted with maleic anhydride (PP-g-MA) is used as compatibilizer (Epolene G-3015, provided by Eastman).

Samples preparation. The nanocomposites were obtained by dilution into the PP matrix of a masterbatch containing the organoclay. The masterbatch (40/40/20 wt%, PP/PP-g-MA/OMMT) was prepared by twin screw extrusion and then diluted into the PP matrix using an internal mixer (Rheocord Haake 600P). The final composition of the nanocomposite investigated was 85/10/5 wt% (PP/PP-g-MA/OMMT). Samples from the internal mixer were compression molded to obtain flat disks with a controlled thickness and diameter.

Rheological characterization. Measurements were performed at 180°C, 200°C and 220°C on an ARES

1

(TA Instruments) rotational rheometer, using a cone and plate geometry, with a cone angle of 0.0401 rad. To minimize the deformation history associated to the preparation and the loading of the sample in the gap, a permanent shear of 1 s^{-1} during 155 s was applied prior to any measurement, to destroy the initial structure and to reach a reproducible steady state [7-8]. Viscoelastic behavior was investigated in the linear domain using a decreasing frequency sweep, from 100 to 0.03 rad/s.

Results and discussions

Time-evolution of the rheological behaviour. Figure 1 presents the variations of the storage modulus G' of the matrix (PP/PP-g-MA) and the nanocomposite after different annealing times (20, 130 and 300 min). As mentioned above, before each annealing, all samples were sheared according to the protocol previously described to obtain a reproducible initial state.
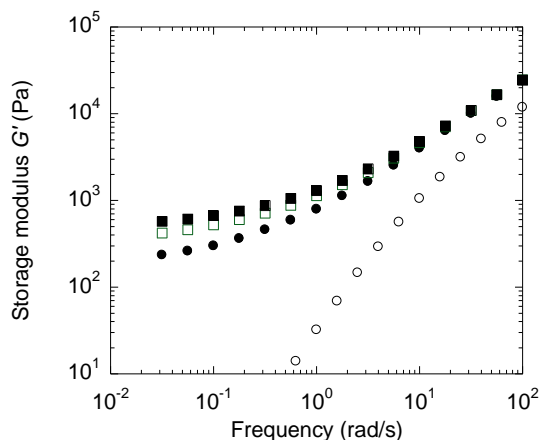

Fig. 1. Variations of storage modulus G' with frequency at 200°C for the matrix (PP/PP-g-MA, ○) and for the nanocomposites annealed at 200°C for 20 min (●), 130 min (□) and 300 min (■).

It can be clearly seen that the nanocomposite exhibits a pronounced low frequency plateau, indicating interactions between the nanofillers (exfoliated platelets and tactoids). This plateau increases with annealing time, indicating that the 3D network is not stable and evolves with time. At high frequency, the contribution of the matrix becomes dominant and the curves superimpose perfectly. According to these observations, it is now interesting to characterize more accurately the time

evolution of the rheological behaviour of the nanocomposite.

Kinetics of the time-evolution of the microstructure. During the pre-shear, the microstructure resulting from the nanocomposite preparation is destroyed, and the platelets and tactoids are oriented in the flow direction. The increase of storage modulus during annealing time is thus attributed to the build-up of a new microstructure. To evaluate the build-up kinetics of this microstructure, measurements were performed on samples at different frequencies and temperatures, using the following protocol. The sample is loaded at a fixed temperature T (180, 200 or 220°C), then sheared for reaching an identical state. Afterwards, the loss and storage moduli are recorded in successive frequency sweeps, between 100 and 0.03 rad/s, for a long period of time (up to 20 h). The thermal stability of the matrix was obviously checked before the experiments.

Figure 2 shows the variations of storage and loss moduli versus frequency for different ageing times. We observe the progressive development of the low frequency plateau on G', whereas a weaker effect can be seen on G''. The perfect superposition of the data at high frequency proves the absence of degradation, even at very long time. We can extract from these data the time evolution of G' for several frequencies (Fig. 3). At high frequency (100 rad/s), G' is stable as it is controlled by the behavior of the polymer matrix. However, when the frequency decreases, the time-evolution of G' is more and more accentuated. Moreover, we can clearly see that this evolution follows a two-step process: above a critical time t_{crit}, situated around 30 000 s, the kinetics is largely accelerated.

Similar time-evolutions of G' were shown by Ren et al. [9] who found a power law evolution, with an experimental exponent between 0.1 and 0.25. To our knowledge, only Treece and Oberhausen [2, 3] reported a two-step process. They found also a time-evolution with two slopes, similar to the ones shown in Fig. 3. Depending on the amount of nanoclay and the preparation procedure, slope values were found between 0.02 and 1.17. In our case, slope values strongly depend on the frequency used for the experiments.
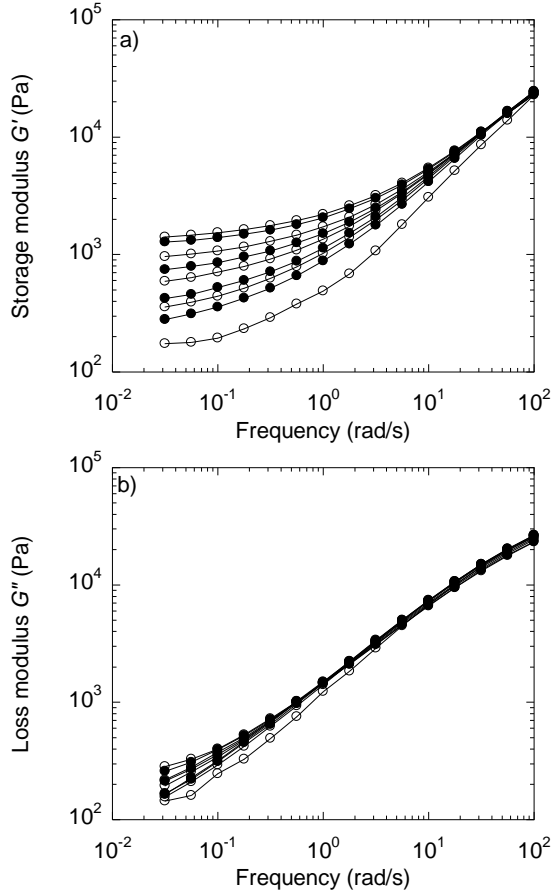
Fig. 2. Time variations of storage modulus G' (a) and loss modulus G'' (b) of the nanocomposite at 200°C. The time increases from bottom to top.
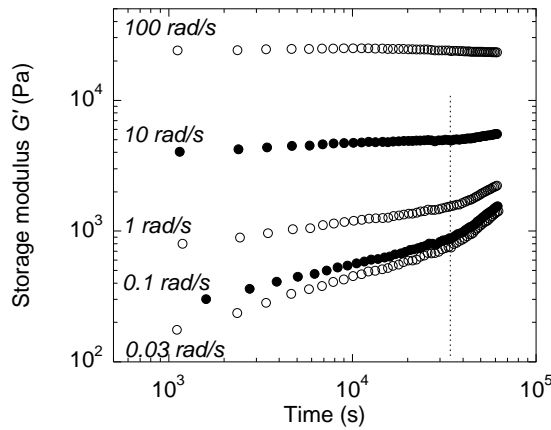

Fig. 3. Time evolution of storage modulus G' for different frequencies at 200°C. The vertical line indicates the critical time where the kinetics changes.

According to Treece and Oberhausen [2, 3], we assume that the first kinetics is related to the disorientation of tactoids and platelets, and the second one to the aggregation of these entities in a 3D network, through Van der Walls attractive forces.

However, it is evident that the description of the kinetics using the slope of G' is inaccurate, as it depends on the frequency. Moreover, this parameter has no physical meaning. To overcome these drawbacks, we suggest to use the complex viscosity curve $\eta^*(\omega)$ and to fit it by a Carreau-Yasuda law with a yield stress [10]:

$$\eta^*(\omega) = \frac{\sigma_0}{\omega} + \eta_0 [1 + (\lambda\omega)^a]^{(n-1)/a} \qquad (1)$$

where σ_0 is the melt yield stress, η_0 the zero-shear viscosity, λ the time constant, a the Yasuda parameter and n the dimensionless power law index. It has been already shown that the value of the melt yield stress σ_0, which is unique and unambiguously defined for a fixed viscosity curve, is a good indicator of the exfoliation level (or more generally of the interactions between the nanofillers) [11-13]. By applying the formalism of Eq. (1) to the data of Fig. 2, we can obtain the values of the yield stress and plot its time-evolution, as shown in Fig. 4. As for the storage modulus, we observe a kinetics in two steps.
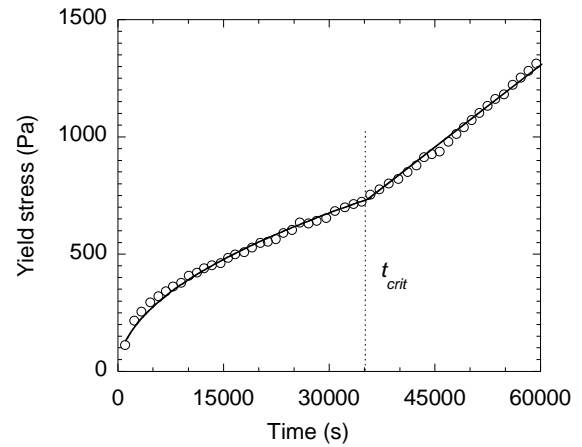

Fig. 4. Time-evolution of the melt yield stress at 200°C. Symbols are experimental data, full lines are theoretical fits using Eqs. (2) and (3).

The first step, attributed to platelets disorientation, can be described by:

$$\sigma_0 = A\sqrt{t} \quad \text{when } t < t_{crit} \qquad (2)$$

3

and the second one, attributed to network aggregation, by:

$$\sigma_0 = A\sqrt{t_{crit}} + B(t - t_{crit}) \text{ when } t > t_{crit} \qquad (3)$$

where A and B are two constants.

As expected, these kinetics are modified by the temperature (Fig. 5): when the temperature increases, the critical time t_{crit} is shorter and both kinetics are accelerated. However, the general form of the kinetics given by Eqs. (2) and (3) remains valid, with A, B and t_{crit} being functions of the temperature.
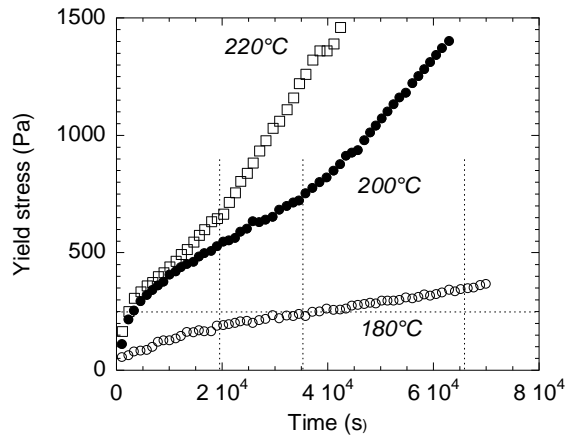

Fig. 5. Time evolution of the yield stress for different temperatures (180°C, 200°C and 220°C). Vertical lines indicate the characteristic times associated to the change in temporal kinetics for the different temperatures. The horizontal line indicates the times associated to the same yield stress for different temperatures.

It is important to notice that, even at very long times, the structure of the nanocomposites does not stabilize. Treece and Oberhausen [2, 3] suggested therefore to consider these materials as belonging to the class of soft colloidal glasses.

Validity of the time-temperature superposition principle. The previous results show that the nanocomposite never reaches a thermodynamically stable state. Therefore, the validity of the TTS principle can be questioned. In a first time, we have tried to apply TTS using an isothermal frequency sweep, after pre-shearing each sample and allowing it to relax for the same period of 20 min. The results obtained are presented on Figure 6. At high frequency, the modulus classically decreases with temperature. But, at low frequency, the level of the plateau increases with the temperature.

Consequently, by shifting the curves along the frequency axis to apply TTS, we obtain a complete failure of this principle. Such behavior was expectable as it is typical for samples whose properties change during the measurements.
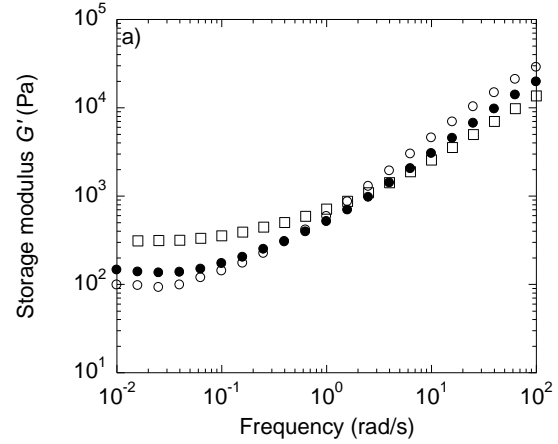

Fig. 6. Variations of storage modulus G' with frequency for three temperatures (□: 220°C ●: 200°C ○: 180°C) at the same annealing time.

We can see in Fig. 5 that, for a fixed annealing time of 20 min, the yield stresses are different according to the temperature, which results into materials having different microstructures. In fact, to correctly apply TTS principle, we have to select, for each temperature, an annealing time providing the same microstructure, i.e. the same yield stress. For example, let us consider the horizontal dotted line in Fig. 5. It indicates that the yield stress obtained after 38 520 s at 180°C (252 Pa) is the same as the one obtained after 3360 s at 200°C and 2160 s at 220°C. The corresponding storage moduli G' are presented in Fig. 7a. If we apply now a frequency shift to these data, using a shift factor a_T, we obtain a perfect mastercurve (Fig. 7b). This time-temperature equivalence indicates that all the processes, including the non-terminal behavior related to the organoclay and also the high frequency relaxations, change with temperature in the same manner. Increasing temperature only accelerates structure build-up and microstructures characterized by the same yield stress are equivalent. The shift factors a_T used to build the mastercurves for the polymer matrix and the nanocomposite are nearly identical, leading to very close values of activation energy (37 kJ/mol). This result implies that the temperature dependence

observed is that of the polymer. Since the silicate layers do not have a temperature dependant relaxation, the only relaxation process is that of the polymer segments.
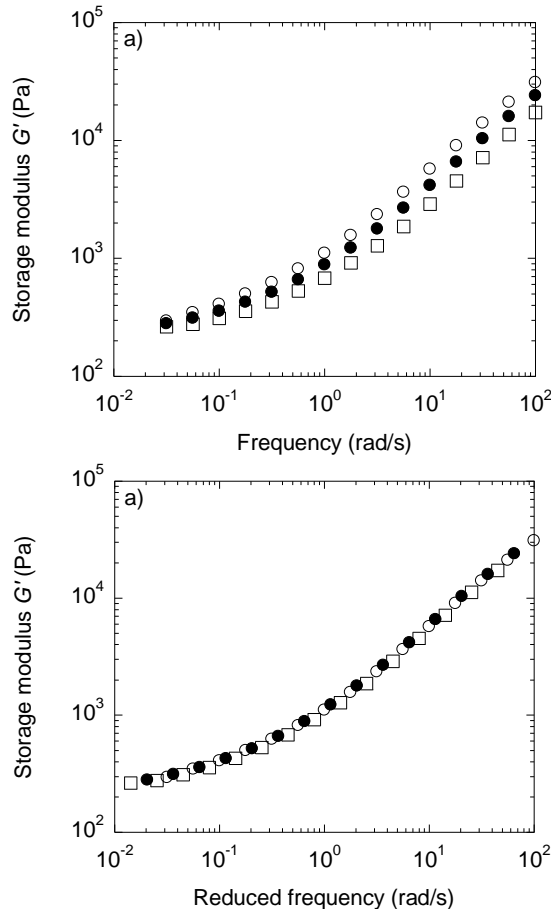

Fig. 7. (a) Variations of storage modulus *G'* with frequency, for three temperatures (□: 220°C ●: 200°C ○: 180°C) and respectively three annealing times (□: 2160 s ●: 3360 s ○: 38 520 s) leading to the same yield stress; (b) Mastercurve of storage modulus *G'* obtained by TTS at 180°C.

Conclusion

We have studied the time-evolution of the storage modulus *G'* of a nanocomposite at different frequencies in oscillatory shear. At high frequency, the polymer matrix controls the behavior and *G'* is almost stable. On the contrary, at low frequency, *G'* presents a monotonic increase with time, associated to the continuous build-up of a structure. We have quantified the kinetics of this structure build-up and shown that it was a two-step process. The first one is attributed to platelets disorientation and the second one, faster, to the aggregation of platelets and tactoids in a 3D network. This structure evolution varies drastically with temperature and, consequently, violates the TTS principle. However, the time-temperature equivalence exists if the samples are annealed for different times, depending on temperature, to obtain similar microstructures, quantified by the same yield stress. This time-temperature equivalence evidences that the behavior of the nanocomposite is governed by the same physical phenomena for the whole temperature range investigated here.

Acknowledgement

References

1.   J. Zhao, A.B. Morgan, J.D. Harris, *Polymer*, **46**, 8641 (2005).
2.   M.A. Treece, P. Oberhauser, *Macromol*., **40**, 571 (2007).
3.   M.A. Treece, Oberhauser, *Polymer*, **48**, 1083 (2007).
4.   P. Reichert, B. Hoffmann, T. Bock, R. Thomann, R. Mullhaupt, C. Friedrich, *Macromol. Rapid Commun*., **22**, 519 (2001).
5.   R. Wagener, T.J.G. Reisinger, *Polymer,* **44**, 7513 (2003).
6.   A.D. Drosdov, E.A. Jensen, J. de C. Christiansen, *Comp. Mat. Sci*., **47**, 807-816 (2010).
7.   W. Lertwimolnun, B. Vergnes, G. Ausias, P.J. Carreau, *J. Non-Newt. Fluid Mech*., **141**, 167 (2007).
8.   A. Reyna-Valencia, Y. Deyrail, M. Bousmina, *Macromol*., **43**, 354 (2010).
9.   J. Ren, A. S. Silva, R. Krishnamoorti, *Macromol*., **33**, 3739 (2000).
10.   B. Vergnes, *Intern. Polym. Proc*., in press (2011).
11.   W. Lertwimolnun, B. Vergnes, *Polymer*, **46**, 3462 (2005).
12.   W. Lertwimolnun, B. Vergnes, *Polym. Eng. Sci*., **46**, 314 (2006).
13.   W. Lertwimolnun, B. Vergnes, *Polym. Eng. Sci*., **47**, 2100 (2007).

5